Correlative study of neutral winds and scintillation drifts measured near the magnetic equator

C. E. Valladares,[1] J. W. Meriwether,[2] R. Sheehan,[1] and M. A. Biondi[3]

Received 9 February 2001; revised 3 October 2001; accepted 7 December 2001; published 18 July 2002.

[1] Measurements of the thermospheric neutral wind at Arequipa, Peru, and observations of the drift of the irregularities at Ancon, Peru, are used to study the coupling that exists between ions and neutrals at equatorial latitudes and the variability of this coupling as a function of the occurrence of scintillations. This study is based on data collected at the Arequipa and Ancon stations between 1996 and 1998. Our comparative analysis indicates that the relative wind-drift values vary depending on season and the solar flux level. We found that during the equinoxes and low solar flux values, the averaged zonal drift is larger than the wind by 15 m s^{-1}, but for solar flux values above 130 units, the average wind exceeds the drift values by 10 to 20 m s^{-1}. We suggest that the occurrence of larger equinoctial drifts can be explained by the existence of altitude gradients in the zonal wind during that season. During the June solstice the zonal wind seems to exceed the irregularity drift by $\sim$10–20 m s^{-1} independent of the solar flux. We also find that the meridional wind shows a modest dependence on the scintillation activity during the June solstice. During scintillation events and between 2000 and 2400 LT the averaged meridional wind observed to the south and north of Arequipa exceeds their corresponding no-scintillation values by 20 m s^{-1}. We present likely explanations of this effect. *INDEX TERMS:* 2415 Ionosphere: Equatorial ionosphere; 2437 Ionosphere: Ionospheric dynamics; 2439 Ionosphere: Ionospheric irregularities; 2427 Ionosphere: Ionosphere/atmosphere interactions (0335); *KEYWORDS:* scintillations, thermospheric wind, irregularity drift, electrodynamics

1. Introduction

[2] Recent studies of equatorial electrodynamics and of spread *F* phenomena have directed attention to the day-to-day variability (weather) of the equatorial thermosphere-ionosphere system, to the strength of the coupling of ions and neutrals in this system, and to the question of how well forecasting the appearance of equatorial spread *F* (ESF) can be achieved given limited access to *F* region parameters by existing ground-based instruments [*Basu et al.*, 1996; *Fejer et al.*, 1999]. Equatorial electrodynamics and the frequency of occurrence of spread *F* accompanied by scintillation activity at UHF frequencies are closely linked. At equatorial latitudes, mostly during quiet conditions, the neutral wind is the main driving force of plasma motion. By producing polarization electric fields through the combined action of the *E* and the *F* region dynamos [*Rishbeth*, 1971a, 1971b], the flow of air from the afternoon pressure bulge transports the equatorial plasma across and along field lines, while changing the altitude of the *F* region peak and the symmetry of the ionospheric density horizontal distribution with respect to the magnetic equator. These two effects make the nighttime *F* layer more or less unstable to the development of the Rayleigh-Taylor instability (RTI). It has long been considered that the equatorial ionosphere is unstable to the RTI mechanism [*Dungey*, 1956; *Woodman and La Hoz*, 1976; *Kelley et al.*, 1976; *McClure et al.*, 1977].

[3] An important feature of equatorial vertical drift morphology is the phenomenon called the pre-reversal enhancement (PRE) [*Woodman*, 1970]. The full development of the PRE has been associated with the sunset decay of the highly conductive *E* layer [*Farley et al.*, 1986] and the reversal of the zonal thermospheric wind from a westward to an eastward direction [*Crain et al.*, 1993]. *Basu et al.* [1996] presented the day-to-day variability of the PRE observed during an extended campaign in South America to suggest that the appearance of a well-developed PRE precedes the onset of ESF. More recently, *Fejer et al.* [1999] have indicated that the magnitude of the vertical plasma drift may constitute the only observable that is required to predict the onset of ESF.

[4] A major question in understanding the several processes that are interlinked with one another in the development of ESF is how the magnitude of the PRE responsible for the rise of the *F* region plasma at evening twilight may be related to the magnitude and direction of the thermospheric wind. The recent work of *Fesen* [1996] has dem-

[1]Institute for Scientific Research, Boston College, Newton Center, Massachusetts, USA.
[2]Department of Physics and Astronomy, Clemson University, Clemson, South Carolina, USA.
[3]Department of Physics and Astronomy, University of Pittsburgh, Pittsburgh, Pennsylvania, USA.

0148-0227/02/2001JA000042$09.00

onstrated the significant effect on equatorial thermospheric dynamics resulting from the penetration of the *F* region by the semidiurnal and diurnal tidal components. The role of such tidal activity is particularly marked in regard to the phenomena of the midnight temperature maximum and the brightness wave [*Colerico et al.*, 1996] seen in the nighttime equatorial airglow.

[5] This paper presents data collected by two instruments: (1) a Fabry-Perot interferometer (FPI) located at Arequipa, Peru (16.5°S, 71.4°W, 3.5°S dip latitude) and (2) a spaced-receiver scintillation interferometer (SRSI) deployed at Ancon, Peru (11.79°S, 77.18°W, 0.9°N dip latitude). Both instruments are currently operating unmanned under the auspices of the CEDAR NSF initiative. The measurements to be discussed here represent the first substantial set of concurrent observations of the neutral wind and the drift of equatorial *F* region irregularities. Two previous investigations based upon short campaign measurements extending over 2 weeks have compared the zonal neutral winds and the *F* region drift of the irregularities [*Basu et al.*, 1991, 1996]. The first paper presented observations of scintillation drifts obtained at Huancayo and zonal neutral winds measured at Arequipa. *Basu et al.* [1991] concluded that scintillation activity was correlated with a well-developed polarization electric field, which leads to a horizontal drift of the *F* region ions equal to that of the neutrals. The second paper presented comparisons of the first set of scintillation drift measurements for the Ancon SRSI with the Arequipa FPI measurements of neutral winds and noted that the day-to-day variability of the zonal thermospheric wind might potentially explain the day-to-day variability of ESF development. The lack of a large number of comparative measurements over an extended period made this conclusion rather tentative. Another study, conducted by *Biondi et al.* [1988], compared the Fabry-Perot neutral winds and the ion drift determined by incoherent scatter techniques at Jicamarca. Two days of simultaneous data found correlated motions of the neutrals and the ionospheric plasma. The present paper extends the simultaneous FPI/SRSI measurements.

[6] Measurements of the thermospheric neutral wind and temperatures at the equatorial station of Arequipa have been conducted since 1983 over one solar cycle. The seasonal and solar cycle dependencies of both zonal and meridional components of the wind have been presented in several publications [*Meriwether et al.*, 1986; *Biondi et al.*, 1990, 1991, 1999]. *Biondi et al.* [1991] demonstrated that the seasonal variations were more pronounced than the solar cycle variations. The averaged meridional winds presented a consistent pattern of southward flows in the early evening, near zero values around midnight and then again southward in the late night. This pattern was typical during the local winter solstice months of May, June, and July. The largest value of the southward meridional wind for solar minimum conditions was $\sim$100 m s^{-1}, which occurred during the early evening. During increased solar activity this peak value decreased by $\sim$10 to 20%. During equinoctial months, meridional winds were $\sim$0 m s^{-1} throughout the night. The zonal winds were found to be almost exclusively eastward during quiet magnetic conditions. The averaged zonal winds exhibited peak values occurring near midnight that increased from $\sim$100 m s^{-1} at solar minimum to $\sim$150–175 m s^{-1} at solar maximum.

[7] More recently, *Meriwether et al.* [1996] have used FPI measurements from Arequipa to show that during solar maximum, the zonal wind is often significantly weaker and the temperature is elevated over the Andes compared to over the Pacific Ocean. The authors suggested that viscous dissipation of waves propagating from below the thermosphere was the causative mechanism of the localized thermospheric heating. A more recent publication [*Meriwether et al.*, 1997] has reinforced the idea of an orographic source as the source of additional energy at longitudes over the Andes.

[8] Throughout this paper we use the term scintillation as synonymous with ESF, although we know that this is not completely accurate. Equatorial spread *F* encompasses a whole array of disturbances that an unstable ionosphere produces for the transmission of radio waves. At equatorial latitudes, plasma turbulence can exist within plasma depletions, which are often called "bubbles" [*Woodman and LaHoz*, 1976]. There also exist bottomside and bottom-type layers [*Hysell and Burcham*, 1998], and volumes containing bottomside sinusoids [*Valladares et al.*, 1983]. Scintillation is the name given to the fading of EM waves (mainly in the UHF and L band range) when signals pass through a turbulent plasma media. For the fading to occur it is necessary that irregularities of scale $\sim$0.1–1 km be present within the usually much larger sized turbulent eddy.

[9] The goals of this paper are the following: (1) to examine, by means of case studies and statistical analysis, the climatology of the zonal and meridional components of the thermospheric wind during scintillation periods and (2) to estimate the degree of coupling that exists between the ions and neutrals during the nighttime hours.

2. FPI and Scintillation Instrumentation

[10] The Arequipa FPI measures nighttime thermospheric winds and temperatures by observing the Doppler shift and spectral broadening of the O I 630.0-nm nightglow emissions. Near the equator at solar minimum the half intensity points of the emitting layer extend over about two scale heights, with the emission centroid at $\sim$255 km [*Meriwether et al.*, 1997]. The altitude of the emission centroid varies between 250 and 285 km, depending on the height of the *F* region and the season of the year. The 630-nm airglow signal detected by the Arequipa FPI instrument is increased by a factor of $\sim$4 through the use of a multiaperture mask [*Biondi et al.*, 1985]. The FPI is refractive index tuned over one free spectral range ($\sim$0.02 nm) by changing the density of argon gas between the plates with a volume changer. The instrument collects a sufficient number of counts after a few minutes of integration to yield measurements of winds and temperature with typical 1-sigma uncertainties of 15 m s^{-1} and $\sim$45 K. The Arequipa FPI usually operates automatically throughout the month, except for a 5-day period centered on the full moon. However, at Arequipa, clear night skies occur regularly only from late March to late October. The night sky for the rest of the year is generally partly cloudy to overcast. Further details regarding the FPI instrument are presented by *Biondi et al.* [1985] and *Meriwether et al.*, [1997].

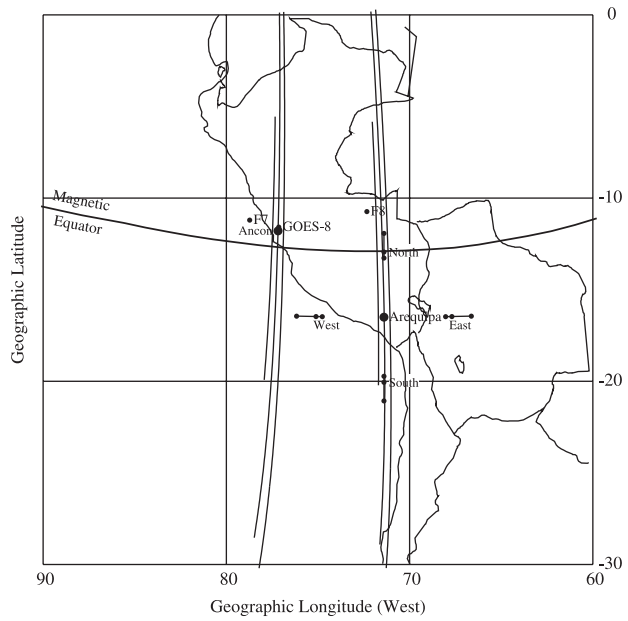

Figure 1. Geometry of the ionospheric and thermospheric observations that operate continuously at Ancon and Arequipa. The large dots indicate the locations of the spaced-receiver scintillation interferometer (SRSI) at Ancon and the Fabry-Perot interferometer (FPI) at Arequipa. The dots labeled F7, GOES 8, and F8 indicate the respective 350-km intersection points for the ray path from Ancon looking west, looking to the GOES 8 satellite, and looking east. The dumbells indicate the horizontal extent of the 630-nm emission between altitudes of 210 and 280 km observed by the FPI for the four cardinal directions, with the internal dots indicating the emission centroids.

[11] Figure 1 shows (1) the locations of the FPI at Arequipa and the SRSI at Ancon (heavy dots), (2) the extension of three field lines with corresponding apex altitudes at 300, 450, and 600 km (light lines), and (3) the latitudinal or longitudinal regions of the airglow observed in determining the averaged Doppler shift in the zonal and meridional directions (bars with dots). The FPI's pointing head is also programmed to observe the 630-nm nightglow layer in the zenith to provide a zero velocity reference for the line-of-sight wind determinations on the assumption that the vertical wind component averaged over one night of observations is small ($\sim$0 m s^{-1}).

[12] At the present time, the Ancon scintillation system receives UHF and L band signals from three geostationary satellites located at 100°W, 75°W, and 20°W longitudes. The system initially consisted of three UHF antennas placed in a magnetic east-west alignment, and a 10-m dish used for L band scintillations. In April 1996 the system was modified to accommodate another baseline consisting of two antennas pointing at 25° elevation to another satellite located at 20° W. Figure 1 displays the geographic locations of the ionospheric intersection point for both baselines and the L band system.

[13] The computer program that controls and processes the data was also upgraded to run in the more robust Labview software environment using a Pentium PC computer. A Linux PC was also incorporated into the system to establish communications, via modem, to a central computer in Lima. This scheme offers near real-time access, via Internet, to selected parameters that can be observed as the experiment progresses.

3. Case Study Comparison of Neutral Wind and Scintillation Drift

[14] Concurrent measurements of scintillation drifts and thermospheric winds have been carried out in the Peru sector since May 1994, when the Ancon SRSI started operations [*Basu et al.*, 1996]. Our study is based on the data collected between the years of 1996 and 1998. Our decision on limiting the database to these years was made because the online software of the SRSI system was not fully calibrated to extract the characteristic velocity (see discussion below about this term). Moreover, the FPI data for the years of 1994 and 1995 required additional processing to remove OH contamination [*Meriwether et al.*, 1997], and, for the purpose of this study, we chose to put aside these results to avoid possible confusion of the statistics developed from the comparison of the zonal neutral winds with the ion drifts.

[15] Before presenting data from the FPI and the scintillation systems, we indicate several sources of error or discrepancies that may exist in measurements from these types of instruments. The scintillation technique measures the transport velocity of 1-km scale irregularities in a plane that is parallel to the antenna layout (magnetic east west) and perpendicular to the local magnetic field line. The field line perpendicularity is the result of the extended elongation of the irregularities in the field line direction. Ideally, the satellite should be located immediately overhead the receiving station in order to measure the east-west horizontal motion of the patch of irregularities. In practice, however, the ray path between the satellite and the receivers will be at an elevation angle, θ, that is less than 90°. At Ancon, the direction to the western satellite is $\sim$65° over the horizon. This introduces a component of the vertical ion drift in the "zonal ion drift" measurements. Since the vertical drift of the equatorial plasma is typically of order 10 m s^{-1} and rarely exceeds 50 m s^{-1}, this relatively small velocity should not significantly alter our measurements of the zonal drifts. However, during magnetically disturbed conditions, plasma bubbles can accelerate from the bottomside and reach supersonic upward speeds in these upward motions. Values as large as 2 km s^{-1} have been reported by *Hanson et al.* [1997] based on in situ measurements by the plasma drift meter instrument mounted on the DE 2 satellite. The 1-km scale irregularities, which are embedded within the large-scale bubbles, may also contain a very significant fraction of this large plasma motion. The new real-time program that controls the spaced receiver instrument is also able to provide the characteristic random velocity V_c. This term gives a measure of the amount of signal decorrelation that exists at two spaced receivers [*Vacchione et al.*, 1987]. The signal decorrelation is produced by quick temporal or spatial changes in the diffraction pattern caused by the turbulent media. It has been noticed that during the early development of a plasma bubble, when its rising motion is the largest and the plasma

turbulence is strongest, the level of V_c exceeds 50 m/s. However, it is much smaller at other times. Consequently, the scintillation technique is able to indicate when a fast, upward moving bubble crosses the ray path and makes it possible to discard such values.

[16] A second source of error is the fact that the scintillation technique measures the speed of ~1-km scale irregularities. This may not be exactly equal to the plasma drift because inside a large bubble a substantial polarization electric field can be created near the walls, which makes the scintillation drift somewhat different than the $\mathbf{E} \times \mathbf{B}$ plasma drift for such bubble events.

[17] Third, there is typically a difference in altitude of approximately one scale height between the two instrument observing volumes. The scintillation drift represents the motion of the irregularities at the height of the peak density of the *F* region. This peak is near 350-km altitude during weak solar activity and will typically be a few tens of kilometers higher for more active periods. The altitude of the line of sight averaged Doppler shift measured by the FPI at Arequipa lies within the bottomside of the F layer; the altitude of the centroid of 630-nm emission varies between 250 and 285 km [*Meriwether et al.*, 1997]. If the wind has a gradient in latitude [*Raghavarao et al.*, 1991] or altitude [*Biondi et al.*, 1999], then a neutral wind measurement at Arequipa may underestimate the actual peak value of the wind by 5 to 10% at the location of the drift measurement. Recently, *Biondi et al.* [1999] has found indirect evidence that suggests the possible existence of a modest vertical gradient in the zonal wind.

[18] We also note that the volumes probed by the scintillation technique and the FPI are not well colocated. The *F* region examined by the scintillation drift receivers and the thermospheric volume probed by the FPI are separated by ~250 km in longitude and ~400 km in latitude.

[19] Operations of the Fabry-Perot instrument are conducted automatically with cloud cover information provided through examination of the images collected by the Boston University (BU) imager system [*Colerico et al.*, 1996]. The FPI results obtained during periods of cloudiness seen in the BU images are discarded. Because the BU imager did not always operate continuously throughout the month, there were times during which FPI observations were obtained without any imager data as to the extent of sky cloudiness. However, our experience has been that for periods of overcast the FPI signals are weak and the apparent Doppler shifts show a large variability. These events are identified easily and discarded. FPI observations for the more marginal situations near the vernal or austral equinoxes were included in our statistical study but excluded in any specific case study comparison. Because the skies are generally clear during the local winter months of May to August, we included these results for which there were no BU 630 nm images in our case studies.

3.1. Scintillation Drift Case Events

[20] Figure 2 shows a set of nearly continuous scintillation drifts measured at Ancon for six nights in September and October 1997. Except for the data of 17/18 September 1997, all other plots of Figure 2 correspond to times of quiet magnetic conditions. Previous measurements of the zonal drift using the incoherent scatter technique [*Fejer et al.*, 1991] or the space receiver technique [*Valladares et al.*, 1996] have indicated that during the early evening the zonal drift becomes eastward and increases. It attains a peak value between 2100 and 2300 local time (LT), and then decreases and reverses during the early morning hours. The equatorial zonal drifts show a great deal of day-to-day variability as seen in the September 1997 data. For example, on 17/18 September the peak value was 150 m s^{-1}, on 18/19 September, 100 m s^{-1}, and on 19/20 September started with a value close to 100 m s^{-1} and then increased to 135 m s^{-1}. On 17/18 September 1997, when the K_p index was 5^0, the zonal drift increased rapidly in the early evening hours, reached a maximum eastward value of 150 m s^{-1}, then decayed to near zero at 0100 LT and reversed at 0310 LT.

[21] The second trace (gray line), shown in some of the frames, is the characteristic velocity V_c. During a typical night V_c is usually well below 50 m s^{-1}, except when the turbulence of the plasma or the upward velocity is large [*Battacharyya et al.*, 1992]. In these cases, as seen in the plots corresponding to 12/13, 13/14, and 14/15 October 1997, the scintillation drifts show large positive or negative spikes and at the same time V_c rises for few minutes above 50 m s^{-1}. As described above, it is quite possible that these spikes correspond to large vertical velocities or shears within the plasma bubbles and are not a zonal $\mathbf{E} \times \mathbf{B}$ drift. As a corollary, we conclude that the V_c parameter can be used to exclude non-$\mathbf{E} \times \mathbf{B}$ drifts by noting when V_c is larger than 50 m s^{-1}. This is a property of our new analysis program that we have exploited.

3.2. Neutral Wind Events During Periods of No Scintillation

[22] Figure 3 shows values of the zonal neutral wind measured at Arequipa on four nights during equinoctial months in 1996 and 1997. The equinoxes are periods when the scintillation activity is strong in the American sector. However, on these specific days, no scintillation events were detected at Ancon. Only a short segment of scintillation appeared in the early morning hours on 23/24 April 1996 (seen on the lower left panel). Each measurement of the zonal neutral wind is plotted with its error bar and a letter (W or E) to indicate the pointing direction of the FPI at the time of the measurement. Similar to the drift measurements, the zonal wind displays a large day-to-day variability in their peak values, time of the peak, width, and rate of decay. The peak value of the winds can be as high as 175 m s^{-1} (23/24 April 1996), or as low as 125 m s^{-1} (19/20 April 1996). On many occasions the zonal winds show a good correlation (equal sign and similar magnitude) in their west and east observations (23/24 April 1996), implying a large degree of longitudinal coherence. At other times the FPI winds show a zonal spatial gradient, which may be an indication of the passage of gravity waves. Also, not all the daily neutral wind patterns exhibit as smooth a growth and decay as the climatological patterns published by *Biondi et al.* [1999] suggest. Instead, as shown on 4/5 and 5/6 October 1996, the zonal wind can decrease in the early evening and then rapidly increase. Such short-term decrease-increase signatures were seen near 1900 LT. It is interesting that on 19/20 April 1996 a magnetically disturbed day ($K_p = 4^-, 4^0$), the zonal wind diminishes from

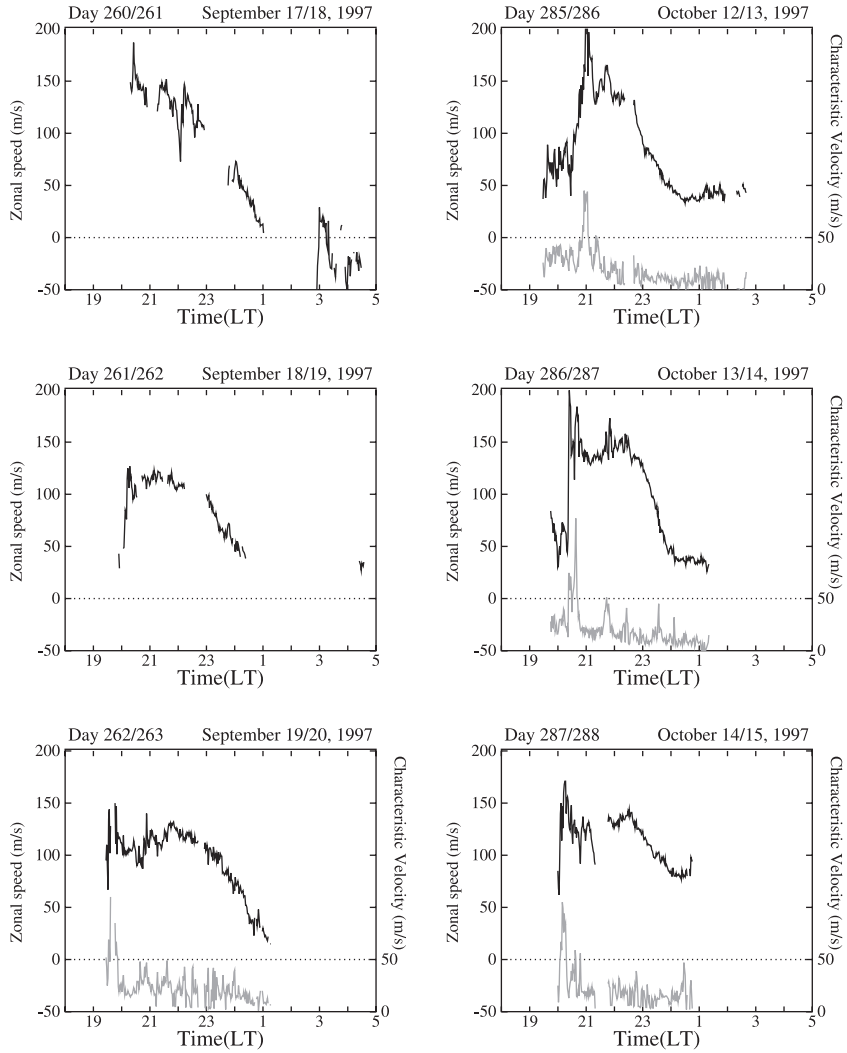

Figure 2. The temporal variation of the scintillation zonal drift (eastward positive) measured at Ancon, Peru, on 6 days during the months of September and October 1997. The gray line at the bottom of some panels displays the characteristic velocity. See text for details.

130 m s^{-1} eastward at 2100 LT to ~0 m s^{-1} westward near 2400 LT. This westward wind value is very reminiscent of the scintillation drifts observed during high K_p values [*Valladares et al.*, 1996].

3.3. Simultaneous Observations of Drifts and Winds

[23] Figures 4, 5, 6, and 7 show several events in which there are concurrent measurements of the neutral winds and the scintillation drifts. Figure 4 shows selected examples obtained during the vernal equinoxes of 1997 and 1998. Two prominent features of these plots are the resemblance that exists between the scintillation drifts and the thermospheric winds, and the longitudinal coherence of the zonal winds. The longitudinal separation between the regions under observation to the east and the west is ~800 km, implying a lack of a gradient over a distance of at least 800 km for the zonal wind. The wind-drift agreement is more evident in the data on 26/27 August 1997, 16/17 October 1998, and 15/16 September 1998. These 3 days qualify as quiet days ($\Sigma K_p < 20$). For the quiet day of 14/15 August 1997, differences of 25–50 m s^{-1} are evident. On this day, there exists also a difference between the zonal winds looking to the east and west at 2400 LT. Some velocity spikes are sometimes seen in the scintillation drifts as on 14/15 August 1997 and 15/16 September 1998. Understandingly, no similar excursions in the neutral winds were seen because of the much coarser temporal resolution of the FPI instrument and because of the likely association of the spikes with rapidly upward drifting bubbles. The negative spikes, such as the ones at 2220 LT on 14/15 August 1997 and at 1940 LT on 15/16 September 1998 correlate with increased values of V_c.

[24] While Figure 4 introduced events of near-zero drift-wind difference; Figures 5, 6, and 7 present more uncommon cases in which the wind-drift difference is >50 m s^{-1} or were obtained in seasons not reported before. Figure 5 shows the scintillation drifts and the zonal winds for two nights during the local autumnal equinoxes of 1996. During this season, there is a reasonable agreement between the winds and drifts. In one of

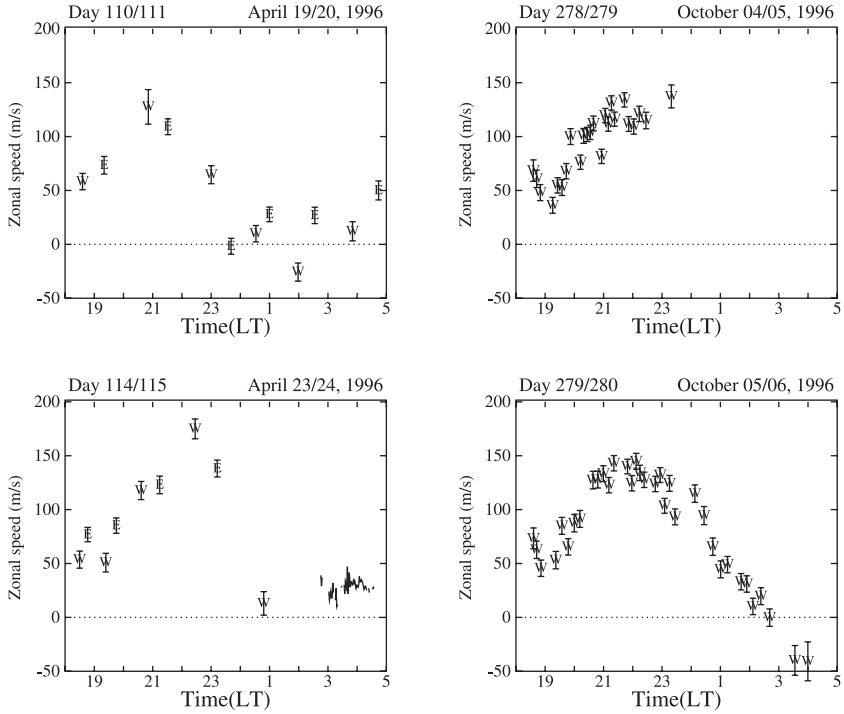

Figure 3. The temporal variation of the zonal neutral winds (eastward positive) measured on four equinoctial nights of 1996. The letters (E) and (W) indicate the observation direction at the time of the measurement. The error bars are also displayed on top of each letter.

the examples (20/21 April 1996), there are drift spikes exceeding 50 m s^{-1}. Not surprisingly, this day is magnetically disturbed, with K_p values >4−. As shown by the gray line in the plot, the large drift values coincide with V_c larger than 50 m s^{-1}.

[25] Figure 6 shows simultaneous drifts and winds measured on two nights during the June solstice. It is known that the scintillation activity is weakest during local winter in the American sector. It occurs only on 10% of the nights, generally after midnight, with a preference for moderate or active magnetic conditions, and in short temporal patches. As seen in the plots, the variability of the wind is increased relative to the observations presented in Figures 3 and 4. Also, the difference in the neutral wind speeds between the east and west directions is significant in several instances.

[26] In Figure 5 we presented two cases where, for 1−2 hours, the wind was equal or larger than the drift. In Figure 7 we present six events in which the FPI wind exceeds the scintillation drift for many hours and in some intervals by ∼50 to 100 m s^{-1}. Most of the nights in Figure 7 (except for 29/30 October 1997) show peak wind values close to 200 m s^{-1}; this is almost twice the average value of the zonal wind for the years analyzed here. The magnetic activity prevailing during these measurements was quiet to moderate with the K_p index varying between 0^O and 3^+. The plots corresponding to 30/31 August 1996, 21/22 September 1998, and 28/29 September 1998 and up to some extent 29/30 October 1997 show a pattern in which the drift curve follows the variation of the wind values with an almost constant difference between them. This signature was commonly observed during most of the nights when wind and drifts were simultaneously measured and gives credence to the good quality of the data. The other two frames, corresponding to 1/2 September 1997 and 5/6 September 1997, present a large difference in the early hours of the evening when the winds exceeded the drifts by near 100 m s^{-1}. This large discrepancy may indicate a lack of coupling between the neutral and the ions. More about this can be found in the discussion section.

4. Statistical Comparison of Neutral Winds and Scintillation Drifts

[27] This section presents the results of a statistical analysis that provided the climatology of the zonal scintillation drifts and the thermospheric winds. We have applied a multivariate regression analysis [*Biondi et al.*, 1999] to both the scintillation drifts and the FPI wind data sets and obtained the dependence of these parameters on the solar flux intensity and the local time. We also calculated average values of the wind for periods of scintillation and no scintillation. We know that by calculating their statistical average we may also remove the day-to-day variability of the wind, which we believe is associated with the onset of the irregularities. We found only a modest difference between the averaged morphologies of both components of the wind when they were sorted according to the presence or absence of scintillations. The 3 years considered in our statistical study correspond to the low and ascending phases of the solar cycle. Between 1996 and 1998, the solar flux varied between 67 and 170 × 10^{-22} W m^{-2} Hz^{-1}. We note that the number of nights considered in our statistical analysis

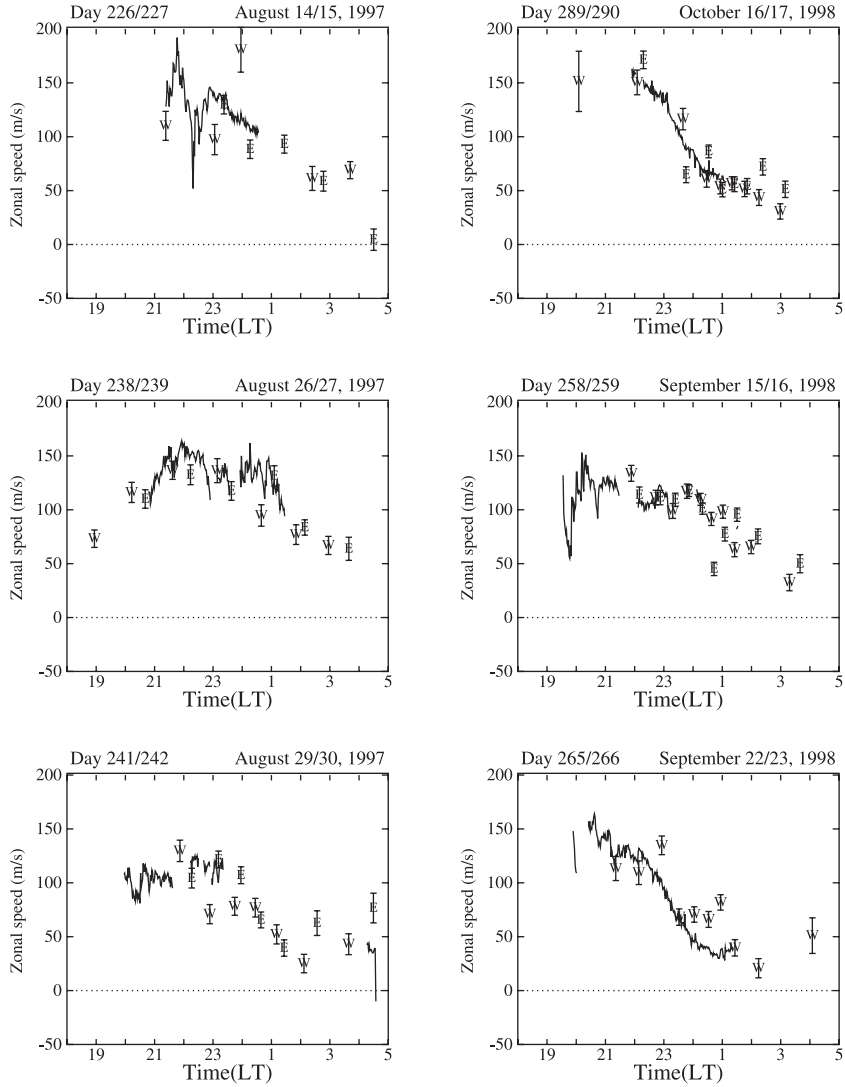

Figure 4. The temporal variation of the scintillation drifts (solid lines) and the neutral winds (symbols E and W, with error bars) measured simultaneously on six nights of the vernal equinox of 1997 and 1998. Note the very good agreement in the values of both data sets.

is relatively small, introducing an inherent statistical uncertainty of order 20 m s^{-1}.

4.1. Climatology of the Coupling Between Neutrals and Plasma

[28] Figure 8 shows the dependence of the irregularity drift and the neutral wind on the local time and the solar flux for the equinoctial months of March, April, September, and October. Figure 9 shows similar variations for the solstitial months of May, June, July, and August. The local time variation of both parameters is quite typical; they increase in the early evening, reach a peak at 2200 LT, and slowly decrease afterward. (Note the heavy line that is used to delineate the 100 m s^{-1} contour.) For the first 5 years of operations of the Ancon SRSI (1994 through 1999), we have systematically reviewed the real-time data of scintillation and drifts. The "quick" format plots that were obtained online reveal that the peak of the nighttime eastward velocity varies proportionally with the intensity of the solar flux. Figure 8a corroborates this statement. Not surprisingly, the peak of the nighttime zonal wind, which is the driver of the nighttime plasma motion at equatorial latitudes, also shows a similar direct proportionality with the solar flux level.

[29] Recently, *Biondi et al.* [1999] have presented the variation of the thermospheric winds measured at Arequipa and Arecibo as a function of solar flux and LT. Arequipa's zonal winds (see their Figure 7) were collected in the previous solar cycle. Although their database extended from 1983 to 1990 and ours is restricted to 1996, 1997, and 1998, the agreement between their Figure 7 and our Figure 8b is very good. In both the peak of the zonal wind occurs at 2200 LT for all values of the solar flux, and the 100 m s^{-1} contour (heavy line) first appears at a solar flux level between 100 and 110.

[30] The prominent feature of Figures 8a and 8b is the fact that in the premidnight period, the scintillation drifts are larger than the zonal winds during low levels of solar flux. This can be seen by comparing the locations of the heavy line contour (corresponding to 100 m s^{-1}) in both

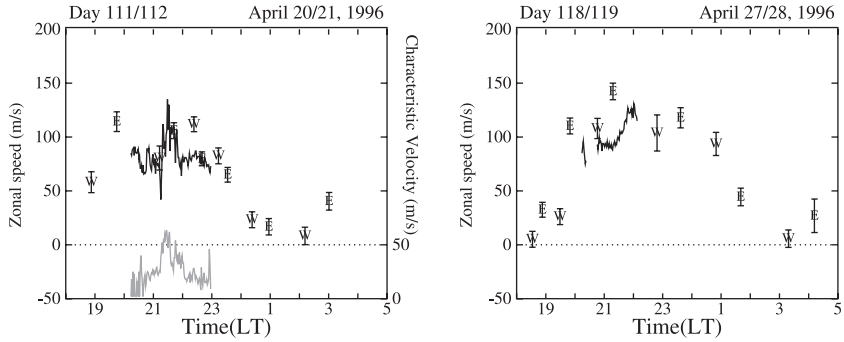

Figure 5. Same format as in Figure 4, but for two nights of the local autumnal equinox of 1996.

panels. Figure 8 indicates that when the solar flux is below 125×10^{-22} W m^{-2}, the drifts are larger than the winds, but for values above ~140, the winds exceed the drifts. This result is somewhat unexpected and may imply the existence of a gradient of the thermospheric wind either in altitude or in latitude. A relatively small difference, probably 20 m s^{-1}, over the latitudinal spacing between Arequipa and Ancon could easily explain the presumed "overdeveloped" scintillation drift found in the scintillation data.

[31] Contrary to the comparative behavior of the winds and drifts for the equinoxes, the wind–drift comparisons of Figures 9a and 9b shows that the premidnight wind values always exceed the drift values during the winter solstice. This relationship is independent of the level of the solar flux during the epoch of low solar flux activity that has been considered in our statistical analysis. The wind's maximum is also broader than the drift's, and the wind contours are further apart, indicating a weaker temporal variation for the winds.

4.2. Climatology of the Meridional Neutral Winds as a Function of Scintillation Activity

[32] Figures 10 and 11 show the meridional component of the thermospheric wind binned as a function of season, scintillation activity and observation directions (north or south). Each individual measurement is represented by a small dot and the half-hour mean average is displayed by the solid line. A salient feature in the average wind values is the roughly constant difference between the meridional winds measured to the north and to the south. For example, the north observations of Figure 11a are near zero between 2000 and 2400 LT. At these times the corresponding south values (Figure 11d) approach 40 m s^{-1}. The north values of Figure 10c are −30 m s^{-1}; the corresponding south values of Figure 10d show near zero wind values after 2200 LT. As explained more extensively in the Discussion section, we believe this persistent difference (wind convergence) implies a latitudinal variability of the meridional wind that exists between the thermospheric volumes observed by the FPI to the north or the south (8° difference in Figure 1). The presence or absence of scintillations also reveals a subtle but interesting effect that occurs during the June solstice (Figures 10a–10d). Figure 10a shows that at 1900 LT the average meridional wind is −45 m s^{-1}, becomes near zero at 2100 LT and then decreases reaching −25 m s^{-1} at 2400 LT. Figure 10b (southward direction) shows an initial meridional wind of −75 m s^{-1} that also decays to zero at 2100 LT, becoming positive afterward. In the case of no scintillations the north-south relation varies quite noticeably. The wind to the north (Figure 10c) is about −42 m s^{-1} at 1900 LT and remains almost unchanged throughout the night. The wind to the south (Figure 10d) starts near −42 m s^{-1}, but rapidly decreases toward zero values (by 2200 LT) and remains near zero. Thus the average meridional winds for scintillation events are less negative, and in some case positive, than their corresponding winds for no scintillation cases. This difference is more significant between 2000 and 2400 LT. There is considerable scatter in the plots of Figure 10 (σ = 15 m s^{-1}), and several counterexamples have been observed. Nevertheless, we find that the meridional wind climatology presents different characteristics for scintillation versus no-scintillation cases that may have some bearing on the onset of scintillation activity or

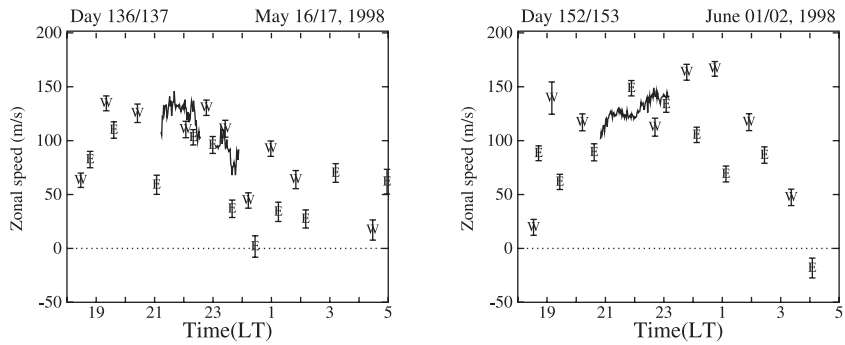

Figure 6. Same format as in Figure 4 but for two nights of the June solstice of 1998.

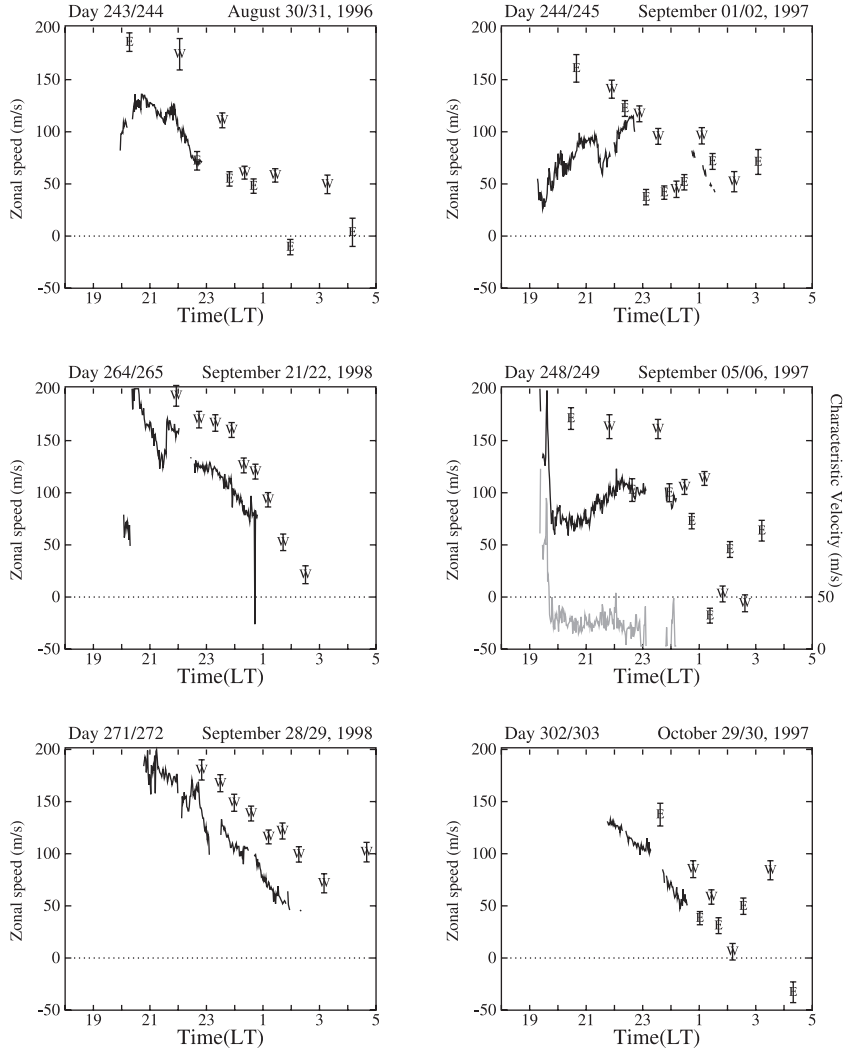

Figure 7. Same format as in Figure 4, but for six nights when the ionospheric plasma motion and the speed of the neutrals were significantly different.

alternatively be a consequence of the development of plasma bubbles and scintillations.

5. Discussion

[33] Comparisons of the plasma drift and neutral wind velocities for the years 1996, 1997, and 1998 have revealed that most often the scintillation drifts and the FPI winds are in good agreement as seen in Figure 4. Both the amplitude and the nighttime trend were almost equal 26/27 August 1997, 15/16 September 1998, 22/23 September 1998, and 16/17 October 1998 (Figure 4). However, on very few occasions the wind and the drift curves differed significantly. These are a small number of cases and no statistical conclusion should be drawn from here. The wind-drift difference sometimes was constant and lasted for several hours, as shown in Figure 7 for 21/22 September 1998 and 28/29 September 1998, or varied, as on 1/2 September 1997 and 5/6 September 1997. The near constant wind and drift difference presented in Figure 7 indicates that even under conditions of incomplete ion-neutral coupling the neutrals can control the motion of the ions from the early evening up to the late night hours. It is known that during the late part of the night, the effect of the *F* region dynamo decreases when the *F* region conductivity becomes comparable to the *E* region conductivity [*Crain et al.*, 1993]. Under these circumstances the ions may not follow the motion of the neutrals, or their velocities may decay more rapidly than the wind. This effect is not apparent in the data of Figure 7.

[34] From Figure 8 it is somewhat surprising to find that during the equinoxes, when the occurrence frequency of scintillations maximizes, in the pre-midnight hours the mean plasma drift exceeds the averaged neutral velocities when the solar flux is below 130 units. This trend reverses for solar flux levels larger than 130.

[35] Other studies have also reported a value of the ionospheric drifts larger than the neutral winds. *Coley et al.* [1994] conducted a systematic comparison of plasma drifts and neutral winds, collected by the DE 2 satellite. Coley et al. used data from the ion drift meter and the wind and temperature spectrometer to show that during the period between 2200 and 0500 LT and at latitudes near the dip equator, the ion drift was larger than the neutral velocity. These authors explained their results, suggesting that an

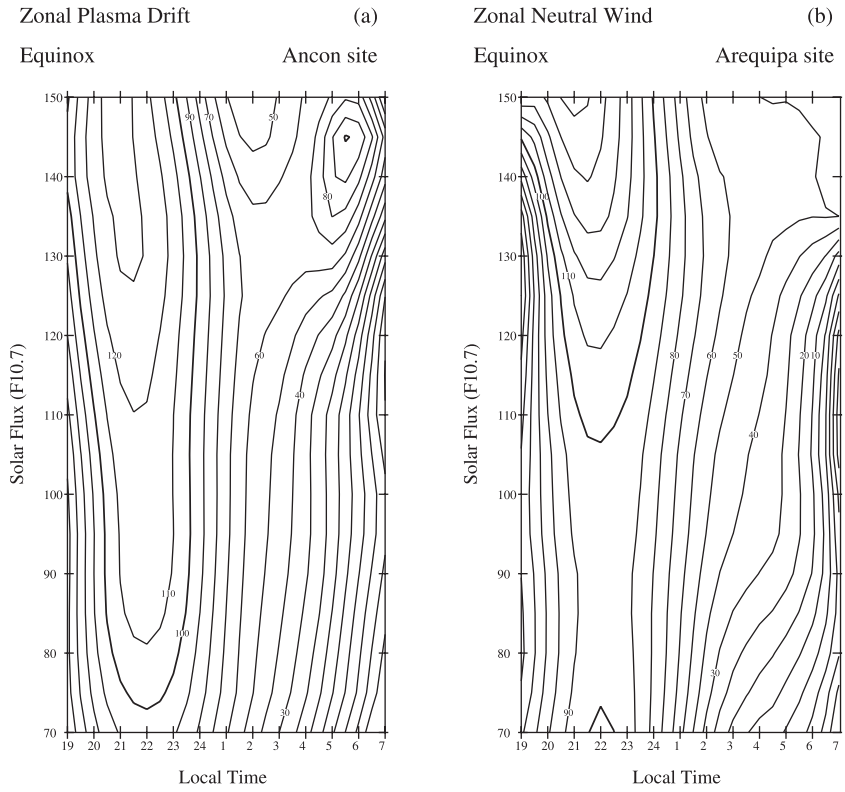

Figure 8. Zonal scintillation drift and zonal thermospheric neutral wind contours obtained by the regression analysis of the data for the equinox periods (March, April, September, and October) of 1996, 1997, and 1998. The dark trace represents a 100 m s^{-1} velocity.

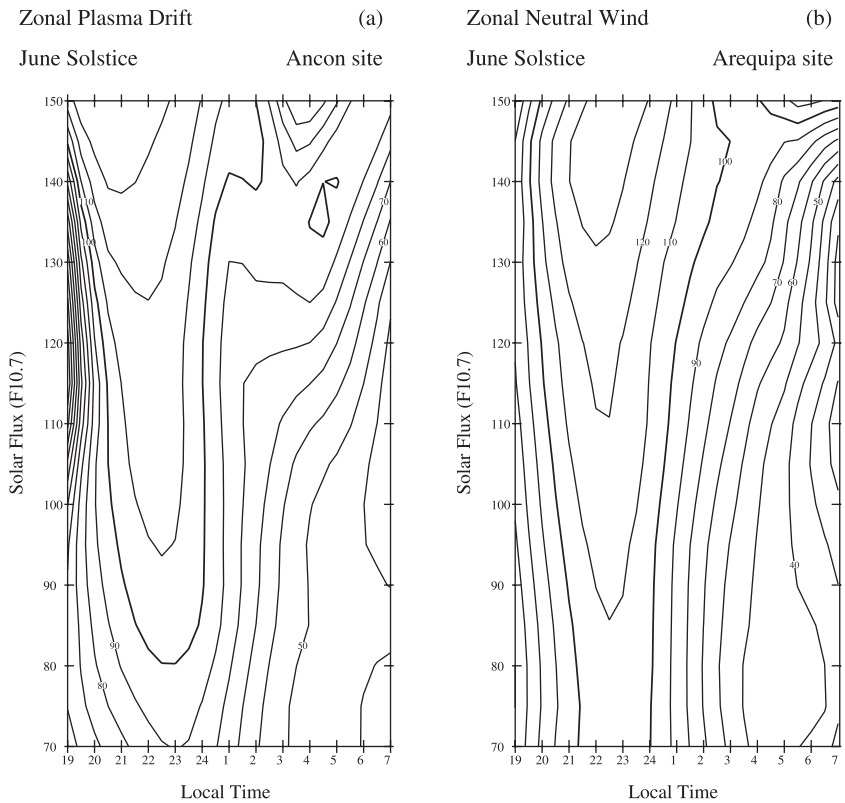

Figure 9. Zonal drift and zonal wind contours calculated using the regression analysis for the local winter solstice (May, June, July, and August).

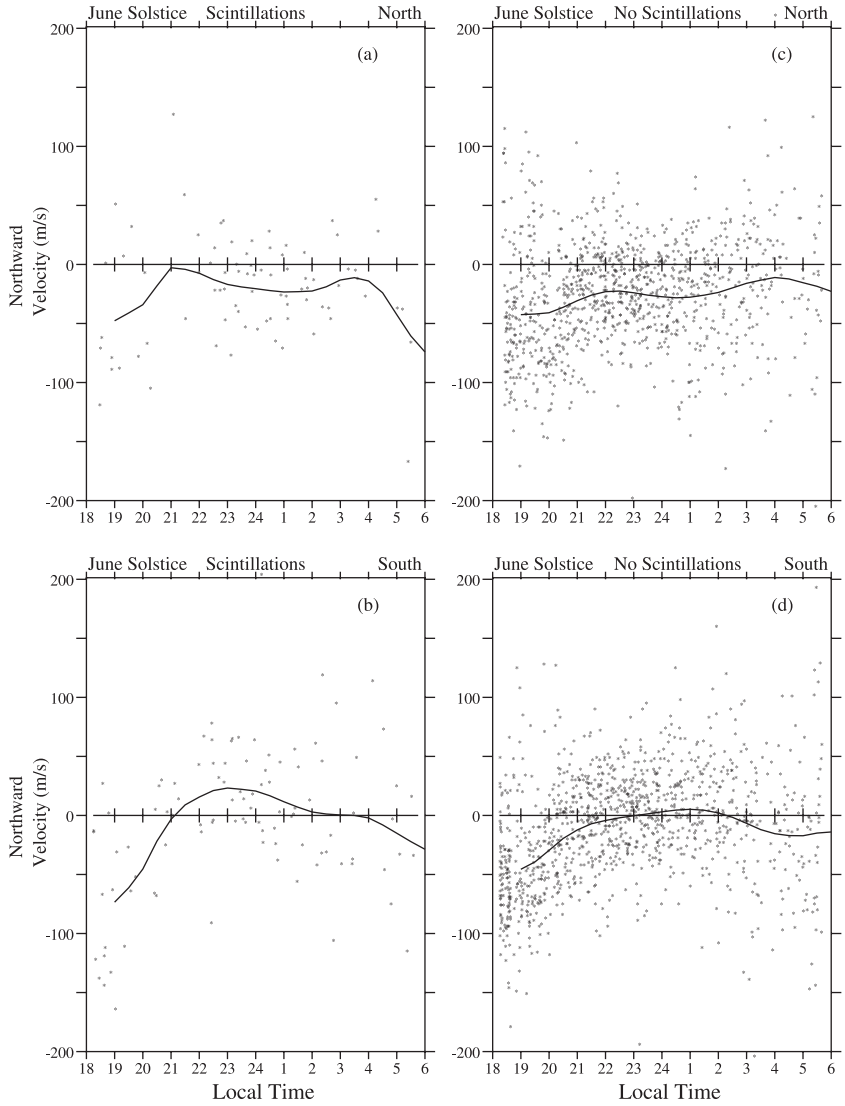

Figure 10. Meridional thermospheric wind (northward positive) measured at Arequipa during the June solstice and displayed according to the observation direction at the time of operation and the presence/absence of scintillations. The smooth curves are fitted to the half−hour mean averages.

additional polarization electric field could be generated by an altitude gradient of the zonal neutral wind in the 100–200 altitude region.

[36] *Basu et al.* [1996] examined concurrent measurements of scintillation drifts and thermospheric winds during a campaign period in 1994. Their observations near sunset indicated large values of the zonal wind during nights of spread *F* compared to smaller winds on other nights of non spread *F* condition. *Basu et al.* [1996] also conducted simultaneous measurements of the scintillation drifts at two different latitudes. In addition to the receivers at Ancon, located near the magnetic equator, they installed another system at Agua Verde at 11° magnetic latitude. The drift measurements at the two sites differed, implying a latitudinal gradient of the wind at *F* region altitudes.

[37] *Anderson and Mendillo* [1983] used a model of the equatorial ionosphere to demonstrate that the westward tilting of the plasma plumes was produced by an altitude decrease of the eastward plasma drift. These authors suggested that the plasma flow gradient was a result of a zonal wind pattern of decreasing speed at increasing distances from the equator. *Raghavarao et al.* [1991] presented zonal wind data measured by the DE 2 satellite when crossing the dip equator, which exhibited a broad maximum centered at the magnetic equator and a minimum at the location of the anomalies. The wind was higher near the equator and decreased by 100 m s^{-1} at both sides toward the poles. A decrease of 50 m s^{-1} was seen even at 12° away from the equator in agreement with the suggestion made by *Anderson and Mendillo* [1983]. *Raghavarao et al.* [1991] explained that the latitudinal distribution of the zonal wind was the result of encountering more dense plasma at the anomalies, which produce a higher ion-drag on the neutrals, and a weaker ionosphere near the equator. Therefore, from the experimental and modeling points of view there is supporting evidence that there exists a latitudinal gradient in the zonal wind in the *F* layer. The fact that we measured drifts larger than the thermospheric wind points also to the

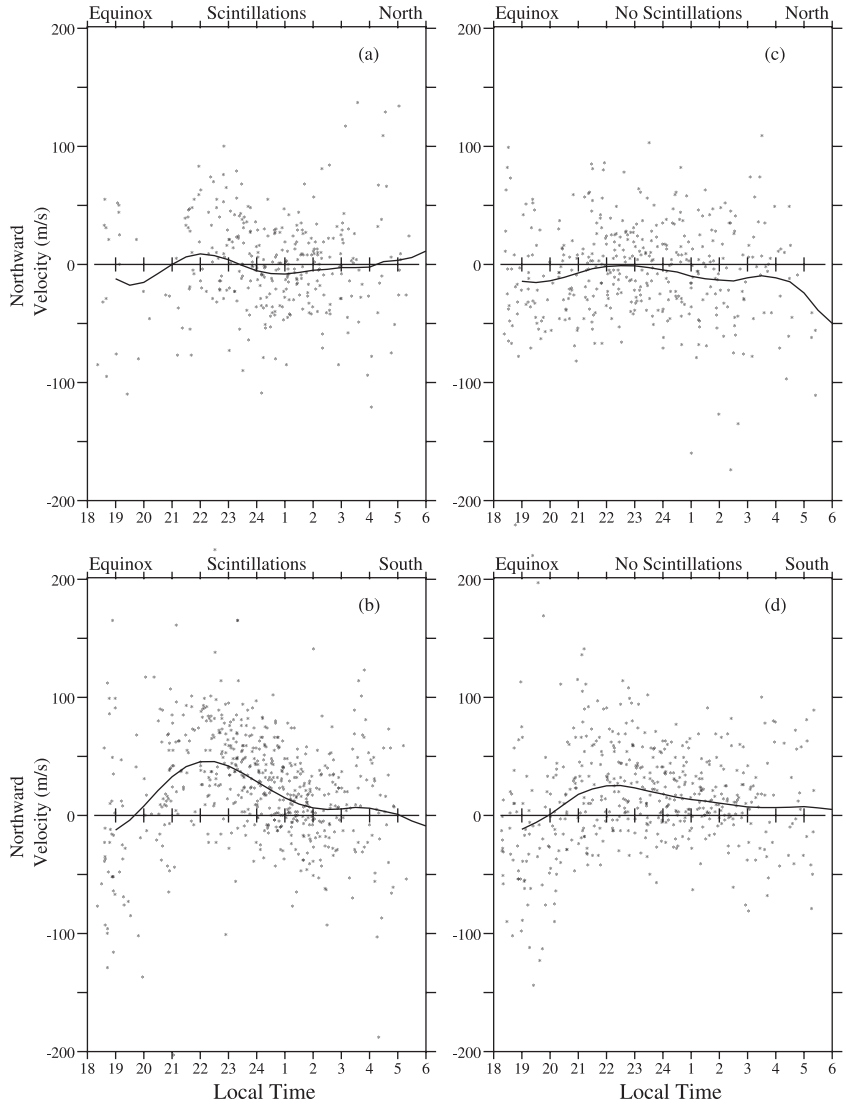

Figure 11. Same as Figure 10, but corresponding to the equinoxes.

existence of a steep latitudinal variability of the neutral wind, or alternatively, the penetration of electric fields originating at higher latitudes.

[38] As described above, the scintillation and the FPI measurements do not correspond to volumes that are collocated; there is a displacement of 50–100 km in altitude, 4° in latitude, and few hundred km in longitude. *Anderson and Mendillo* [1983] and *Anderson et al.* [1987] showed that the drift is related to an integrated conductivity, while the wind could be more localized depending on the thermospheric tides, heat sources, and to a lesser degree, interaction with the local ionosphere. Wind-drift differences like the ones encountered on 21/22 September 1998 and 28/29 September 1998 could be explained by the existence of sharp gradients in altitude/latitude and longitude. However, on others days (1/2 September 1997 and 5/6 September 1998) the wind-drift differences were of order 100 m s^{-1}, with the winds exceeding the drifts. We believe that for these events, penetrating electric fields extending from high to low latitudes may play a role in creating a larger downward electric field [*Fejer et al.*, 1979; *Spiro et al.*, 1988; *Sastri et al.*, 1993]. We have seen on other days (e.g., 20/21 April 1996 of Figure 5) that the zonal wind hardly reaches a peak magnitude of 100 m s^{-1}. The wind seems reduced throughout the night. This significantly reduced wind can be attributed to the presence of a disturbed dynamo.

[39] In the cases presented in Figure 7, we observed several occasions when the wind exceeded the drifts. While it is undeniable that a latitudinal gradient of the wind can explain the smaller drifts, an underlying conductive *E* layer persisting after sunset could also produce smaller drifts by partially shorting out the polarization *E* field. However, the fact that the measured wind-drift difference remains almost constant for many hours would require the persistence of the *E* region during the night. This weak *E* region should be able to damp the growth of the Rayleigh-Taylor instability and consequently inhibit the occurrence of scintillation, which did not occur.

[40] A wind distribution of large eastward values near the magnetic equator, where the ion drag is reduced, and much smaller wind values near the latitudes of both anomalies (see, for example, Figure 6 of *Richmond* [1995]) could well

produce the signature seen in our measurements. Figure 8 suggests that the ion drifts were slightly larger than the neutral winds during solar minimum conditions. During these conditions the ionosphere should be located at lower altitudes and able to exert a higher ion drag effect than during solar maximum conditions. For the solar-moderate epoch we observed almost equal wind and drift values, suggesting the absence of altitude gradients in the wind. Another common feature in the wind data is the spatial variability that accompanied the more dramatic cases in which the wind-drift difference was the largest.

5.1. Effect on Zonal Wind During Scintillation Events

[41] We have observed that, during scintillation and solar minimum conditions (e.g., solar flux levels below 120), the nighttime zonal wind presented a pattern of eastward winds sometimes increasing in magnitude shortly after sunset. The zonal wind of 1/2 June 1998 and 16/17 May 1998 (Figure 6) show this feature. *Crain et al.* [1993] showed that a west-to-east wind reversal and/or a positive altitude gradient of the zonal wind are able to increase the zonal polarization electric field (and generate a more fully developed PRE) that lifts the *F* layer, thereby making the *F* layer more unstable. It seems that for solar minimum the *F* layer needs a bit larger prereversal enhancement, as could be obtained by the combined action of the decay of the *E* region conductivity and the rapidly increasing eastward zonal wind. During solar maximum conditions, when the *F* region densities are higher, the conductivity gradient may be large enough to generate a significant PRE able to lift the equatorial ionosphere toward higher, more unstable altitudes. A large PRE in the vertical velocity (or an equivalent eastward electric field) is an important factor in the growth of the RTI for three reasons: (1) it lifts the *F* region to altitudes where the stabilizing damping collisional term is smaller; (2) it produces an eastward electric field, which is also a destabilizing term in the generalized RTI; and (3) it helps to decrease the integrated Pedersen conductivity of the field line connected *E* region [*Hanson et al.*, 1983, 1986].

5.2. On a Possible Association Between Meridional Winds and Scintillations

[42] We have observed that the presence/absence of scintillations produced a tenuous effect, but still identifiable, on the characteristics of the meridional wind when we obtained the statistics of the winds independently of the FPI observation directions. During no scintillation periods and the June solstice the averaged meridional winds to the north and south have both an average value of about -40 m s^{-1} in the early part of the evening ($\sim$1900 LT). During scintillation events and also the June solstice season, the meridional winds to the south were more negative with an average value of -75 m s^{-1} at 1900 LT compared to -40 m s^{-1} to the north. It was also observed that the average wind was less negative or even positive until 2300 LT during nights of scintillations than during nights when scintillations were absent. The statistical significance of our conclusion is reduced due to the limited number of scintillation days that were recorded during the June solstice. Between years 1996 and 1998 the Arequipa FPI measured the meridional winds on 125 nights during the June solstices. Of these, only 30 nights contained some level of scintillations. This low percentage of scintillation activity is quite common in the American sector during the June solstice.

[43] The meridional wind at *F* region altitudes results from and/or is modified by the action of several agents. During geomagnetically quiet conditions, local heating due to solar radiation is a principal source that prevails even near local sunset. During more disturbed conditions, however, there exists a disturbed dynamo, which is able to initiate a transequatorial meridional wind that can reach wind speeds of order 100 m s^{-1}. *Fuller-Rowell et al.* [1994, 1996] used a coupled thermosphere-ionosphere model to illustrate how the meridional wind develops after the initiation of a magnetic storm and diminishes after penetrating into the opposite hemisphere. The midnight temperature maximum (MTM) can also modify substantially the value of the meridional wind. Either of the latter two factors may reduce or even cancel the meridional wind in a region near the magnetic equator. Consequently, as can be seen by reference to Figure 1, Arequipa observations to the north ($\sim$0° dip latitude) and to the south ($\sim$8° S dip latitude) could differ, depending on the importance of these mechanisms.

[44] Finally, for completeness we mention a third possibility, that our results might be a consequence of the development of a local circulation cell system as advocated by *Raghavarao et al.* [1991, 1993, 1998]. The analysis by *Pant and Sridharan* [2001] suggests that both chemical heating and ion drag mechanisms operating within the Appleton anomaly crests generate the dynamical forcing that produces this convective cellular activity. *Raghavarao et al.* [1998] based their supposition for this local circulation cell upon the analysis of Dynamic Explorer in situ measurements of zonal and vertical winds with a mass spectrometer. This work found an indication of reduced zonal winds within the Appleton anomaly, upward vertical wind above the anomaly crests, and increased zonal winds and downward vertical winds at the magnetic equator. It was also noted that continuity requires increased meridional wind flow within the thermosphere from the crests of the Appleton anomaly to the equator and return meridional flow within the *E* region to complete the cellular circulation. During the winter solstice such winds would be difficult to detect against the background flow of air from the summer hemisphere to the winter hemisphere that is generated by the pressure gradient between the two hemispheres. During the equinoxes, because of the reduced global pressure gradient, this interhemispheric transport should be nearly zero. We note that the observed increase of equatorward winds observed to the south as compared with the north for periods of increased scintillation activity are consistent with this mechanism. A recent study based upon eight nights of simultaneous measurements made during 2 weeks in late September and early October 1997 (C. Martinis et al., Zonal neutral winds at equatorial and low latitudes, submitted to *Journal of Geophysical Research*, 2001) has demonstrated a $\sim$15–20% reduction in the zonal wind between Arequipa and Carmen Alto; a reduction that is

consistent with the idea of a local circulation cell presented by *Raghavarao et al.* [1998].

6. Conclusions

[45] This work has led to the following conclusions:

1. The amplitudes of the scintillation zonal drifts and the thermospheric neutral winds are often in good agreement; in addition, their nighttime temporal variations correlate well. This implies that the zonal polarization electric field produced by the nighttime *F* region dynamo is fully developed, generating a perfect electrodynamical coupling.

2. On a few occasions, especially during low solar activity, the plasma drift is found to be larger than the zonal wind. We suggest that on these days there exists a significant vertical gradient of the horizontal wind with lower values at the bottomside of the *F* region, where the winds are observed, and significantly larger wind values close to the *F* region peak, where the scintillation drifts are measured. On very few nights did we find that the wind was substantially larger than the drift (>100 m s^{-1}). We believe that on these nights the *E* region may be sufficient to short out some of the polarization electric field that drives the zonal plasma drift but still allow *F* region irregularities to develop.

3. The meridional winds measured to the north and to the south of Arequipa during the June solstice were binned independently according to the scintillation activity. The results plotted in Figure 11 show that during the equinoxes, when there is scintillation activity, the averaged meridional wind measured either to the south or north of Arequipa during the mid-evening hours is more equatorward by 20–30 m s^{-1} than the wind observed during nights with no scintillation activity. Little difference in the meridional wind speeds was noted for the winter solstice period. Use of two FPI interferometers located on the same side of the magnetic equator (Arequipa, Peru, and Carmen Alto, Chile), should make it possible to provide a better determination of the latitudinal distribution of the zonal and meridional components of the neutral wind. In our future work we intend to explore the possibility that the correlation between scintillation activity and the amplitudes of the zonal and meridional components of the neutral wind is a result of the formation of a neutral wind cell as suggested by *Raghavarao et al.* [1991, 1993]. The mechanism proposed suggested that the combination of chemical and ion drag heating within the Appleton anomaly would reduce the zonal wind flow and produce upward vertical winds at the latitude of the Appleton anomaly, and downward vertical winds at the magnetic equator. Converging meridional flow from the Appleton anomalies to the magnetic equator within the thermosphere would connect these two vertical branches of the convective circulation cell. We will study this phenomenon further in analyses of our results from Arequipa and Ancon during the solar maximum period, 2000–2001.

[46] **Acknowledgments.** We thank Jorge Espinoza and Ruben Villafani for their dedication in operating continuously the spaced receiver scintillation instrument at Ancon, Peru. The research at Boston College was funded by NSF grant ATM-9714804 and by Air Force Research Laboratory contract F19628-97-C-0094, at Clemson University by NSF grant ATM-9714770, and at the University of Pittsburgh by NSF grant ATM-9414403 and ATM-9906408. The Observatory of Ancon is operated by the Instituto Geofisico del Peru, Ministry of Education. Space and on-site technical support at Arequipa, Peru are provided by the National Aeronautics and Space Administration.

[47] Janet G. Luhmann thanks Donald T. Farley and another referee for their assistance in evaluating this paper.

References

Anderson, D. N., and M. Mendillo, Ionospheric conditions affecting the evolution of equatorial plasma depletions, *Geophys. Res. Lett.*, *10*, 541, 1983.

Anderson, D. N., R. A. Heelis, and J. P. McClure, Calculated nighttime eastward plasma drift velocities at low latitudes and their solar cycle dependence, *Ann. Geophys., Ser. A*, *5*, 435, 1987.

Basu, S., Su. Basu, E. Kudeki, H. P. Zengingonul, M. A. Biondi, and J. W. Meriwether, Zonal irregularity drifts and neutral winds measured near the magnetic equator in Peru, *J. Atmos. Terr. Phys.*, *53*, 743, 1991.

Basu, S., et al., Scintillations, plasma drifts, and neutral winds in the equatorial ionosphere after sunset, *J. Geophys. Res.*, *101*, 26,795, 1996.

Bhattacharyya, A., K. C. Yeh, and S. J. Franke, Deducing turbulence parameters from transionospheric scintillation measurements, *Space Sci. Rev.*, *61*, 335, 1992.

Biondi, M. A., D. P. Sipler, and M. Weinschenker, Multiple aperture exit plate for field-widening a Fabry-Perot interferometer, *Appl. Opt.*, *24*, 232, 1985.

Biondi, M. A., J. W. Meriwether, B. G. Fejer, and R. Woodman, Measurements of the dynamics and coupling of the equatorial thermosphere and the *F*-region ionosphere in Peru, *J. Atmos. Terr. Phys.*, *50*, 937, 1988.

Biondi, M. A., J. W. Meriwether, B. G. Fejer, and S. A. Gonzalez, Seasonal variations in the equatorial thermospheric wind measured at Arequipa, Peru, *J. Geophys. Res.*, *95*, 12,243, 1990.

Biondi, M. A., J. W. Meriwether, B. G. Fejer, S. A. Gonzalez, and D. C. Hallenbeck, Equatorial thermospheric wind changes during the solar cycle: Measurements at Arequipa, Peru, from 1983 to 1990, *J. Geophys. Res.*, *96*, 15,917, 1991.

Biondi, M. A., S. Y. Sazykin, B. G. Fejer, J. W. Meriwether, and C. G. Fesen, Equatorial and low latitude thermospheric winds: Measured quiet time variations with season and solar flux from 1980 to 1990, *J. Geophys. Res.*, *104*, 17,091, 1999.

Colerico, M., M. Mendillo, D. Nottingham, J. Baumgardner, J. Meriwether, J. Mirick, B. Reinish, J. Scali, and C. Fesen, Coordinated measurements of *F*-region dynamics related to the thermospheric midnight temperature maximum, *J. Geophys. Res.*, *101*, 26,783, 1996.

Coley, W. R., R. A. Heelis, and N. W. Spencer, Comparison of low-latitude ion and neutral zonal drifts using DE 2 data, *J. Geophys. Res.*, *99*, 341, 1994.

Crain, D. J., R. A. Heelis, G. J. Bailey, and A. D. Richmond, Low-latitude plasma drifts from a simulation of the global atmospheric dynamo, *J. Geophys. Res.*, *98*, 6039, 1993.

Dungey, J. W., Convective diffusion in the equatorial *F* region, *J. Atmos. Terr. Phys.*, *9*, 304, 1956.

Farley, D. T., E. Bonnelli, B. G. Fejer, and M. F. Larsen, The prereversal enhancement of the zonal electric field in the equatorial ionosphere, *J. Geophys. Res.*, *91*, 13,723, 1986.

Fejer, B. G., C. A. Gonzales, D. T. Farley, M. C. Kelley, and R. F. Woodman, Equatorial electric fields during magnetically disturbed conditions, 1, The effect of the interplanetary magnetic field, *J. Geophys. Res.*, *84*, 5797, 1979.

Fejer, B. G., E. R. de Paula, S. A. Gonzalez, and R. F. Woodman, Average vertical and zonal F region plasma drifts over Jicamarca, *J. Geophys. Res.*, *96*, 13,901, 1991.

Fejer, B. G., L. Scherliess, and E. R. de Paula, Effects of the vertical plasma drift velocity on the generation and evolution of equatorial spread *F*, *J. Geophys. Res.*, *104*, 19,859, 1999.

Fesen, C. G., Simulation of the low latitude midnight temperature maximum, *J. Geophys. Res.*, *101*, 26,683, 1996.

Fesen, C. G., G. Crowley, R. G. Roble, A. D. Richmond, and B. G. Fejer, Simulation of the pre-reversal enhancement in the low latitude vertical ion drifts, *Geophys. Res. Lett.*, *27*, 1851, 2000.

Fuller-Rowell, T. J., M. V. Codrescu, R. J. Moffett, and S. Quegan, Response of the thermosphere and ionosphere to geomagnetic storms, *J. Geophys. Res.*, *99*, 3893, 1994.

Fuller-Rowell, T. J., M. V. Codrescu, H. Rishbeth, R. J. Moffett, and S. Quegan, On the seasonal response of the thermosphere and ionosphere to geomagnetic storms, *J. Geophys. Res.*, *101*, 2343, 1996.

Hanson, W. B., S. Sanatani, and T. N. L. Patterson, Influence of the *E* region dynamo on equatorial spread *F*, *J. Geophys. Res.*, *88*, 3169, 1983.

Hanson, W. B., B. L. Cragin, and A. Dennis, The effect of vertical drift on the equatorial *F*-region stability, *J. Atm. Terr. Phys.*, *48*, 205, 1986.

Hanson, W. B., W. R. Coley, R. A. Heelis, and A. Urquhart, Fast equatorial bubbles, *J. Geophys. Res.*, *102*, 2039, 1997.

Hedin, A. E., et al., Revised global model of thermospheric winds using satellite and ground-based observations, *J. Geophys. Res.*, *96*, 7657, 1991.

Hysell, D. L., and J. D. Burcham, JULIA radar studies of equatorial spread *F*, *J. Geophys. Res.*, *103*, 29,155, 1998.

Kelley, M. C., G. Haerendel, H. Kappler, A. Valenzuela, B. B. Balsley, D. A. Carter, W. L. Ecklund, C. W. Carlson, B. Hausler, and R. Torbet, Evidence for a Rayleigh-Taylor type instability and upwelling of depleted density regions during equatorial spread *F*, *Geophys. Res. Lett.*, *3*, 448, 1976.

McClure, J. P., W. B. Hanson, and J. H. Hoffman, Plasma bubbles and irregularities in the equatorial ionosphere, *J. Geophys. Res.*, *82*, 2650, 1977.

Meriwether, J. W., J. W. Moody, M. A. Biondi, and R. G. Roble, Optical interferometric measurements of nighttime equatorial thermospheric winds at Arequipa, Peru, *J. Geophys. Res.*, *91*, 5557, 1986.

Meriwether, J. W., J. L. Mirick, M. A. Biondi, F. A. Herrero, and C. G. Fesen, Evidence for orographic wave heating in the equatorial thermosphere at solar maximum, *Geophys. Res. Lett.*, *23*, 2177, 1996.

Meriwether, J. W., M. A. Biondi, F. A. Ferrero, C. G. Fesen, and D. C. Hallenbeck, Optical interferometric studies of the nighttime equatorial thermosphere: Enhanced temperatures and zonal wind gradients, *J. Geophys. Res.*, *102*, 20,041, 1997.

Pant, T. K., and R. Sridharan, Plausible explanation for the equatorial temperature and wind anomaly (ETWA) based on chemical and dynamical processes, *J. Atmos. Sol. Terr. Phys.*, *63*, 885, 2001.

Raghavarao, R., L. E. Wharton, N. W. Spencer, H. G. Mayr, and L. H. Brace, An equatorial temperature and wind anomaly (ETWA), *Geophys. Res. Lett.*, *18*, 1193, 1991.

Raghavarao, R., W. R. Hoegy, N. W. Spencer, and L. E. Wharton, Neutral temperature anomaly in the equatorial thermosphere: A source of vertical winds, *Geophys. Res. Lett.*, *11*, 1023, 1993.

Raghavarao, R., R. Suhasini, W. R. Hoegy, H. G. Mayr, and L. Wharton, Local time variation of equatorial temperature and zonal wind anomaly (ETWA), *J. Atmos. Sol. Terr. Phys.*, *60*, 631, 1998.

Rishbeth, H., The *F* layer dynamo, *Planet. Space Sci.*, *19*, 263, 1971a.

Rishbeth, H., Polarization fields produced by winds in the equatorial *F* region, *Planet. Space Sci.*, *19*, 357, 1971b.

Richmond, A. D., Modeling equatorial ionospheric electric fields, *J. Atmos. Terr. Phys.*, *57*, 1103, 1995.

Sastri, J. H., J. V. S. Visweswara Rao, and K. B. Ramesh, Penetration of polar electric fields to the nightside dip equator at times of geomagnetic sudden commencements, *J. Geophys. Res.*, *98*, 17,517, 1993.

Spiro, R. W., R. A. Wolf, and B. G. Fejer, Penetration of high-latitude electric-field effects to low latitudes during SUNDIAL 1984, *Ann. Geophys.*, *6*, 39, 1988.

Vacchione, J. D., S. J. Franke, and K. C. Yeh, A new analysis technique for estimating zonal irregularity drifts and variability in the equatorial F region using spaced receiver scintillation data, *Radio Sci.*, *22*, 745, 1987.

Valladares, C. E., W. B. Hanson, J. P. McClure, and B. L. Cragin, Bottomside sinusoidal irregularities in the equatorial *F*-region, *J. Geophys. Res.*, *88*, 8025, 1983.

Valladares, C. E., R. Sheehan, S. Basu, H. Kuenzler, and J. Espinoza, The multi-instrumented studies of equatorial thermosphere aeronomy scintillation system: Climatology of zonal drifts, *J. Geophys. Res.*, *101*, 26,839, 1996.

Woodman, R. F., Vertical drift velocities and east-west electric fields at the magnetic equator, *J. Geophys. Res.*, *75*, 6549, 1970.

Woodman, R. F., and C. LaHoz, Radar observations of *F* region equatorial irregularities, *J. Geophys. Res.*, *81*, 5447, 1976.

M. A. Biondi, Department of Physics and Astronomy, University of Pittsburgh, Pittsburgh, PA 15260, USA.

J. W. Meriwether, Department of Physics and Astronomy, Clemson University, Clemson, SC 29631, USA.

R. Sheehan and C. E. Valladares, Institute for Scientific Research, Boston College, Newton Center, MA 02215, USA.